

Statistical Mechanics of Low-Density Parity Check Error-Correcting Codes over Galois Fields

Kazutaka Nakamura¹(), Yoshiyuki Kabashima¹() and David Saad²()

¹Department of Computational Intelligence and Systems Science, Tokyo Institute of Technology, Yokohama 2268502, Japan.

²The Neural Computing Research Group, Aston University, Birmingham B4 7ET, UK.

(received ; accepted)

PACS. 89.90+n { Other areas of general interest to physicists.

PACS. 89.70+c { Information science.

PACS. 05.50+q { Lattice theory and statistics; Ising problems.

Abstract. { A variation of low density parity check (LDPC) error correcting codes defined over Galois fields $(GF(q))$ is investigated using statistical physics. A code of this type is characterised by a sparse random parity check matrix composed of C nonzero elements per column. We examine the dependence of the code performance on the value of q , for finite and infinite C values, both in terms of the thermodynamical transition point and the practical decoding phase characterised by the existence of a unique (ferromagnetic) solution. We find different q -dependencies in the cases of $C = 2$ and $C = 3$; the analytical solutions are in agreement with simulation results, providing a quantitative measure to the improvement in performance obtained using non-binary alphabets.

Error correction mechanisms are essential for ensuring reliable data transmission through noisy media. They play an important role in a wide range of applications from magnetic hard disks to deep space exploration, and are expected to become even more important due to the rapid development in mobile phones and satellite-based communication.

The error-correcting ability comes at the expense of information redundancy. Shannon showed in his seminal work [10] that error-free communication is theoretically possible if the code rate, representing the fraction of informative bits in the transmitted codeword, is below the channel capacity. In the case of unbiased messages transmitted through a Binary Symmetric Channel (BSC), which we focus on here and which is characterized by a bit flip rate p , the code rate $R = N/M$ which allows for an error-free transmission satisfies

$$R < 1 - H_2(p); \quad (1)$$

() knakamura@fedistitech.ac.jp

() kaba@distitech.ac.jp

() saadd@aston.ac.uk

Table I. { Sum (left) and product (right) in GF (4).

L	0	1	2	3
0	0	1	2	3
1	1	0	3	2
2	2	3	0	1
3	3	2	1	0

N	0	1	2	3
0	0	0	0	0
1	0	1	2	3
2	0	2	3	1
3	0	3	1	2

where $H_2(p) = -p \log_2 p - (1-p) \log_2 (1-p)$, when both lengths of the original message N and the codeword M become infinite. The right hand side of (1) is often termed Shannon's limit.

Unfortunately, Shannon's derivation is non-constructive and the quest for practical codes which saturate this limit has been one of the central topics in information theory ever since. The current most successful code in use is arguably the Turbo code [1], although the best performance to date, in terms of proximity to Shannon's bound for a particular rate, has been achieved by variations of the low-density parity check (LDPC) code, proposed by Gallager [3].

A variation of Gallager's code has been recently discovered independently by McKay and Neal [7]; an irregular construction of this code, using a non-binary alphabet, provides the best error correction performance to date [2]. This discovery, based on improving the code construction and the alphabet used by trial and error, instigated the current work, aimed at clarifying the role played by the alphabet used in obtaining this outstanding code performance. To separate the effect of code irregularity from that of the alphabet used we focus here on the dependence of regular constructions on the chosen alphabet. To some extent this complements our previous investigation on the impact of code irregularity on the system's performance [13] in the case of binary alphabets.

Using a non-binary alphabet based on Galois fields GF(q) is carried out in the following manner: The sender first converts the Boolean message vector \mathbf{B} of dimensionality N where $\mathbf{B}_i \in \{0,1\}$; $8i$, to an N/b dimensional vector of GF($q = 2^b$) elements; where each segment of b consecutive bits is mapped onto a GF(q) number⁽¹⁾. The GF(q) vector is then encoded to an M/b dimensional GF(q) codeword \mathbf{z}_0 , in the manner described below, which is then reconverted to an M dimensional Boolean codeword \mathbf{z}_0^B , transmitted via a noisy channel. Corruption during transmission can be modelled by the noise vector \mathbf{B} , where corrupted bits are marked by the value 1 and all other bits are zero, such that the received corrupted codeword takes the form $\mathbf{z}^B = \mathbf{z}_0^B + \mathbf{B} \pmod{2}$. The received corrupted Boolean message is then converted back to a GF(q) vector \mathbf{z} , and decoded in the GF(q) representation; finally the message estimate is interpreted as a Boolean vector.

Firstly, we briefly explain the mapping of binary vectors onto the Galois field GF(q) elements. These represent a closed set of elements which can be added and multiplied utilizing an irreducible polynomial composed of Boolean coefficients. For instance, the irreducible polynomial for GF(4) is $x^2 + x + 1$. Then, identifying the $b (= 2)$ components of the binary vector with Boolean coefficients of a b 1 degree polynomial, $3 = (x+1) + 1 \pmod{2} = x + 2$ and $3 = (x+1) \cdot x \pmod{2} = 1 \pmod{2} = 1$, setting $x^2 + x + 1 = 0 \pmod{2}$. Table I summarises the sum and product operations in Galois field GF(4). Secondly, we explain

⁽¹⁾ Binary vectors will be denoted by a superscript B ; other vectors are in the GF(q) representation.

the encoding/decoding mechanism using regular LDPC code in the GF (q) representation. This is based on a randomly constructed sparse parity check matrix A of dimensionality $(M \times N) = b \times M = b$. This matrix is characterised by C and K nonzero GF (q) elements per column/row. The choice of C, K is linked to the code rate R , obeying the relation $C = K = 1/R$.

Nonzero elements in each row are independently and randomly selected from a specific distribution that maximises the entropy of the vector A (all operations of vectors in the GF (q) representation will be carried out as defined for this field; for brevity we do not introduce different symbols to denote these operations) when \mathbf{a} is the GF (q) representation of the binary random noise vector \mathbf{B} . Then, one constructs an $M \times b \times N \times b$ generator matrix G^T , which is typically dense, satisfying $AG^T = 0 \pmod{q}$.

Using this matrix, encoding is carried out in the GF (q) representation by taking the product $z_0 = G^T \mathbf{a}$; encoding is performed by taking the product of the parity check matrix A and the received corrupted message $z = z_0 + \mathbf{n}$, which yields the syndrome vector $J = Az = A\mathbf{n}$. The most probable estimate of the noise vector \mathbf{n} is defined using the equation

$$A\mathbf{n} = J; \quad (2)$$

via the iterative method of Belief Propagation (BP) [7]. This has been linked, in the case of Boolean codes, to the TAP (Thouless, Anderson, Palmer) based solution of a similar physical system [5], a relation which holds also in the case of GF (q) codes as will be shown elsewhere.

The noise vector estimate is then employed to remove the noise from the received codeword and retrieve the original message by solving the equation $G^T \mathbf{a} = z - \mathbf{n}$.

The similarity between error-correcting codes and physical systems was first pointed out by Sourlas in his seminal work [11], by considering a simple Boolean code, and by mapping the code onto well studied Ising spin systems. We recently extended his work, which focused on extensively connected systems, to the case of finite connectivity [5]. Here, we generalise these connections to spin systems in which the interaction is determined using the GF (q) algebra.

In order to facilitate the current investigation, we first map the problem to that of a GF (q) spin system of finite connectivity. The syndrome vector J is generated by taking sums of the relevant noise vector elements $J = A_{i_1 i_1} + \dots + A_{i_K i_K}$, where $\mathbf{a} = (a_i)_{i=1, \dots, M=b}$ represents the true channel noise; the indices i_1, \dots, i_K correspond to the nonzero elements in i -th row of the parity check matrix $A = (A_k)$. It should be noted that the noise components a_i are derived from a certain distribution $P_{pr}(a_i)$, representing the nature of the communication channel; this will serve as our prior belief to the nature of the corruption process. This implies that the most probable solution of Eq. (2) corresponds to the ground state of the Hamiltonian

$$H(\mathbf{n}) = \sum_{i_1, i_2, \dots, i_K} D_{i_1 i_2, \dots, i_K} \delta(J_{i_1 i_2, \dots, i_K} - A_{i_1} n_{i_1} - \dots - A_{i_K} n_{i_K}) - \sum_{i=1}^{M=b} \ln P_{pr}(n_i); \quad (3)$$

in the zero temperature limit $\beta \rightarrow \infty$. Elements of the sparse tensor $D_{i_1 i_2, \dots, i_K}$ take the value 1 if all the corresponding indices of parity matrix A are nonzero in some row i , and 0 otherwise. The last expression on the right relates to the prior probability of the noise vector elements. Note that operations between vectors/elements in the GF (q) representation (e.g., within the δ function) are carried out as defined in this field.

The delta function provides 1 if the contribution for the selected site $A_{i_1} n_{i_1} + \dots + A_{i_K} n_{i_K}$ is in agreement with the corresponding syndrome value $J_{i_1 i_2, \dots, i_K}$, recording an error, and 0 otherwise. Notice that this term is not frustrated as there are $M=b$ degrees of freedom while only $(M \times N) = b$ constraints arise from Eq. (2), and its contribution can therefore vanish at sufficiently low temperatures. The choice of $\beta \rightarrow \infty$ imposes the restriction (2), limiting the

solutions to those for which the first term of (3) vanishes, while the second term, representing the prior information about the noise, survives.

The optimal estimator, minimizing the expectation of discrepancy per noise bit, is of the form $\mathbf{b}_i = \arg \max_{\mathbf{a} \in \mathbb{F}_2^q} h(\mathbf{n}_i; \mathbf{a})$. This is known as the marginal posterior maximiser (MPM) [4] and corresponds to the finite temperature decoding at Nishimori's temperature studied in other codes [2, 9, 8]. Notice that here, due to the hard constraints imposed on the dynamical variables, decoding at zero temperature is optimal, as the true posterior distribution (given \mathbf{J}) relates to the ground state of Hamiltonian (3), similar to other LDPC codes [6]. The macroscopic quantity $m = \langle b_i \rangle = \frac{1}{M} \sum_{i=1}^M \langle b_i \rangle$ serves as the performance measure.

To eliminate the dependency of the syndrome $J_{h_{i_1}, \dots, i_K}$ on the noise vector we employ the gauge transformation $n_i \rightarrow n_i + i$, $J_{h_{i_1}, \dots, i_K} \rightarrow 0$. Rewriting Eq. (3) in this gauge moves the dependency on i to the second term where it appears in a decoupled form $(-1)^{n_i + i} \ln P_{pr}(n_i + i)$. The remaining difficulty comes from the complicated site dependency caused by nontrivial $\mathbb{F}_2(q)$ algebra in the first term. However, one can rewrite this dependency in a simpler form

$$\langle 0; A_{i_1} n_{i_1} + \dots + A_{i_K} n_{i_K} \rangle = \langle 0; A_1 a_1 + \dots + A_K a_K \rangle \quad (4)$$

$A_1, \dots, A_K; a_1, \dots, a_K = 0$

$$(A_1; A_{i_1}) \dots (A_K; A_{i_K}) \quad (a_1; n_{i_1}) \dots (a_K; n_{i_K});$$

by introducing K Roncker's and the dummy variables A_1, \dots, A_K and a_1, \dots, a_K .

Since codes of this type are usually used for long messages with $N = 10^3 - 10^5$, it is natural to resort to the methods of statistical mechanics for analysing their properties. The random selection of sparse tensor \mathbf{D} , identifying the nonzero elements of \mathbf{A} , and the noise vector introduces quenched disorder to the system. More specifically, we calculate the partition function $Z(\mathbf{D}; \mathbf{A};) = \text{Tr}_n \exp[-H]$ averaged over the disorder and the statistical properties of the noise estimation, using the replica method [5, 6]. Taking $n \rightarrow 1$ gives rise to a set of order parameters

$$Q_{a_1; a_2, \dots, a_n} = \frac{1}{M} \sum_{i=1}^M \langle Z_i \rangle^n \quad h(a; n_i) \quad (5)$$

$\mathbf{D}; \mathbf{A};$

where $n = 1, \dots, n$ represents the replica index and a runs from 0 to $q-1$, and the variables Z_i come from enforcing the restriction of C connections per index i

$$\langle Z_i \rangle^n = \frac{1}{C} \int \prod_{h_{i_2}, \dots, i_K} dC_{h_{i_2}, \dots, i_K} \quad \frac{dZ}{Z} \quad h_{i_2}, \dots, i_K \quad h_{i_2}, \dots, i_K \quad (C+1) \quad (6)$$

To proceed further, one has to make an assumption about the symmetry of order parameters. The assumption made here is that of replica symmetry reflected in the representation of the order parameters and of the related conjugate variables:

$$Q_{a_1; a_2, \dots, a_n} = \int dP \quad (P_0, \dots, P_{q-1}) \quad P_a \quad (7)$$

$$\phi_{a_1; a_2, \dots, a_n} = \int d\mathbf{p} \quad (\mathbf{p}_0, \dots, \mathbf{p}_{q-1}) \quad \mathbf{p}_a$$

where a_0 and $a_{\mathbf{p}}$ are normalisation coefficients; (P) and \mathbf{p} represent probability distributions for q dimensional vectors $\mathbf{P} = (P_0, \dots, P_{q-1})$ and $\mathbf{p} = (\mathbf{p}_0, \dots, \mathbf{p}_{q-1})$, respectively.

Unspecified integrals are performed over the region $P_0 + \dots + P_{q-1} = 1, P_a = 0, \dots, q-1 = 0$ or $P_0 + \dots + P_{q-1} = 1, P_a = 0, \dots, q-1 = 0$. Extremizing the averaged expression with respect to the probability distributions, one obtains the following free energy per spin

$$\begin{aligned} \frac{b}{M} \ln Z_{D, A} = & \text{Ext}_{\{P, b\}} : \sum_{l=1}^q \sum_{a=0}^{q-1} P_a^l \ln \left[\sum_{a=0}^{q-1} P_{pr}(a+l) \right] \\ & + \frac{C}{K} \sum_{l=1}^q \sum_{a_1, \dots, a_K=0}^{q-1} \ln \left[\sum_{a=0}^{q-1} P_{a_1}^l \right] \\ & - C \sum_{a=0}^{q-1} P_a \ln P_a; \end{aligned} \quad (8)$$

where \bar{h}_A and \bar{h}_i denote averages over the distribution of nonzero units per row in constructing the matrix A and over $P_{pr}()$, respectively.

One can calculate the free energy via the saddle point method. Solving the equations obtained by varying Eq.(8) is generally difficult. However, it can be shown analytically that a successful solution

$$P_a = (P_0 - 1) \sum_{a=1}^{q-1} P_a; \quad b(P) = (P_0 - 1) \sum_{a=1}^{q-1} P_a; \quad (9)$$

which implies perfect decoding $m = 1$, extremizes the free energy for $C \geq 2$. For $C \leq 1$, an unsuccessful solution, which provides $m < 1$, is also obtained analytically

$$P_a = \sum_{a=0}^{q-1} P_a P_{pr}(a+l); \quad b(P) = \sum_{a=0}^{q-1} P_a \frac{1}{q}; \quad (10)$$

Inserting these solutions into (8) it is found that the solution (9) becomes thermodynamically dominant with respect to (10) for $R < 1 - H_2(p)$ independently of q ; which implies that the code saturates Shannon's limit for $C \leq 1$ as is reported in the information theory literature [2].

Finding additional solutions analytically is difficult, we therefore resorted to numerical methods. Approximating the distributions P_a and $b(P)$ by 5×10^3 - 3×10^4 sample vectors of P and P we obtained solutions by updating the saddle point equations (100 - 500 iterations) for codes of connectivity $C = 2, \dots, 6$ and GF (q) representation $q = 2, 4, 8$ and for both BSC and Gaussian channels. Less than 50 iteration were typically sufficient for the solutions to converge. Due to lack of space we present here results only for the case of the BSC; results for the case of Gaussian channels are qualitatively similar and will be presented elsewhere.

Since the suggested properties are different for $C \geq 3$ and $C = 2$, we describe the results separately for the two cases. For $C \geq 3$, it turns out that Eq.(9) is always locally stable. However, an unsuccessful solution, approaching (10) as $C \rightarrow 1$, becomes thermodynamically dominant for sufficiently large input rate p . As the noise level is reduced, the solution (9) becomes thermodynamically dominant at a certain input rate $p = p_c$, and remains dominant until $p \rightarrow 0$. This implies that perfect decoding $m = 1$ is feasible for $p < p_c$. However, the locally stable unsuccessful solution remains as well above a certain noise level $p_s(p_c)$.

As $C \rightarrow 1$, the transition point p_c converges from below to Shannon's limit $p_c = 1 - H_2(1 - R)$ irrespective of the value of q . For finite C , p_c monotonically increases with q but does not saturate p_c . This implies that error correcting ability of the codes when optimally decoded is monotonically improved as q increases.

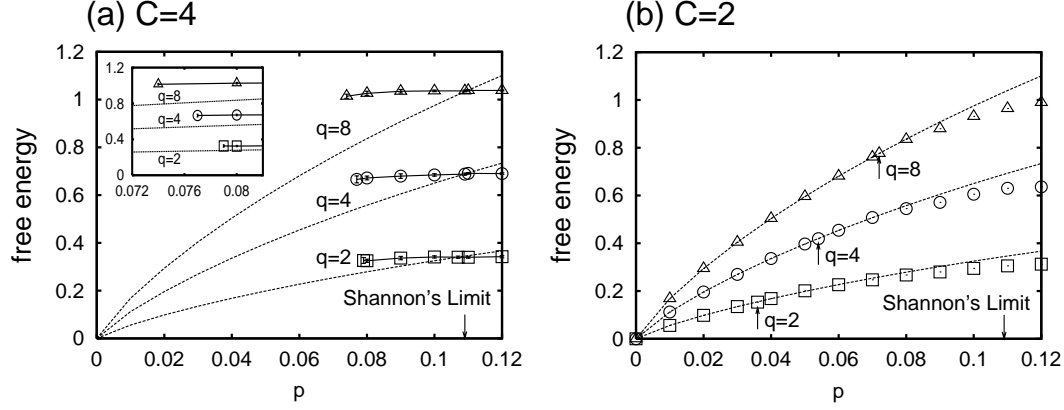


Fig. 1. { Extremised free energies (8) obtained for $q = 2; 4; 8$ as functions of the bit rate p (a) for connectivity $C = 4$ (3) and (b) for $C = 2$ codes with the same code rate $R = 1$, $C = K = 1/2$. In both codes, broken lines represent free energies of successful solution (9), while markers stand for unsuccessful solutions ($m < 1$). Monte Carlo methods with $5 \cdot 10^3$ – $3 \cdot 10^4$ samplings at each step are employed for obtaining the latter with statistical fluctuations smaller than the symbolsize. For each q value, the solution having the lower free energy becomes thermodynamically dominant. In (a), crossing points provide the critical bit rate for p_c being $0.106; 0.108$ and 0.109 (within the numerical precision) for $q = 2; 4$ and 8 , respectively, monotonically approaching Shannon's limit $p_s = H^{-1}(1/2) = 0.109$. The inner figure focuses on the vicinity of the spinodal points p_s , determining the limit of successful practical decoding. This shows p_s to decrease with increasing q . (b) shows that $C = 2$ codes exhibit continuous transitions between the successful and unsuccessful solutions. The critical bit rate p_b , pointed by arrows, is increases with q , while it is still far from Shannon's limit.

The behaviour of the spinodal point p_s is quite different, as shown in Fig. 1a, presenting the dependence of p_c and p_s on q for connectivity $C = 4$ (3). It appears that p_s is generally decreasing with respect to q (except for unique pathological cases), indicating a lower practical corruption limit for which BP/TAP decoding will still be effective. Above this limit BP/TAP dynamics is likely to converge to the unsuccessful solution due to its dominant basin of attraction [6]. In contrast, $C = 2$ codes exhibit a different behaviour; the solution (9) becomes the unique minimum of free energy (8) for sufficiently small noise levels, which implies that practical decoding dynamics always converges to the perfect solution. However, as the noise level increases, the solution loses its stability and continuously bifurcates to a stable suboptimal solution. Unlike the case of $C = 3$, this bifurcation point p_b , which monotonically increases with q , determines the limit of practical BP/TAP decoding. The practical limit obtained is considerably lower than both Shannon's limit and the thermodynamic transition point p_c for other $C = 3$ codes with the same q value (Fig. 1b). Therefore, the optimal decoding performance of $C = 2$ codes is the worst within this family of codes.

However, p_b can become closer to, and even higher than, the spinodal point p_s of other $C = 3$ codes for large q values, (Table II) implying that the practical decoding performance of $C = 2$ codes is not necessarily inferior to that of $C = 3$ codes. This is presumably due to the decreasing solution numbers to Eq. (2) for $C = 2$ as q increase, compared to the moderate logarithmic increase in the information content, tipping the balance in favour of the perfect solution. This may shed light on the role played by $C = 2$ elements in irregular constructions.

Table II. { The critical noise level, below which BP/TAP-based decoding works successfully, for different connectivity values C in the case of $q = 8$ and $R = 1 - C/K = 0.5$. This is determined as the spinodal point p_s and the bifurcation point p_b for $C = 3$ and $C = 2$, respectively. The critical noise for $C = 2$ becomes higher than that of $C = 3$.

C	2	3	4	5	6
Critical noise	0.072	0.088	0.073	0.062	0.050

In summary, we have investigated the properties of LDPC codes defined over GF(q) within the framework of statistical mechanics. Employing the replica method, one can evaluate the typical performance of codes in the limit of infinite message length. It has been shown analytically that codes of this type saturate Shannon's limit as $C \rightarrow 1$ irrespective of the value of q , in agreement with results reported in the information theory literature [2]. For finite C , numerical calculations suggest that these codes exhibit two different behaviours for $C = 3$ and $C = 2$. For $C = 3$, we show that the error correcting ability of these codes, when optimally decoded, is monotonically improving as q increases; while the practical decoding limit, determined by the emergence of a suboptimal solution, deteriorates. On the other hand, $C = 2$ codes exhibit a continuous transition from optimal to sub-optimal solutions at a certain noise level, below which practical decoding dynamics based on BP/TAP methods converges to the (unique) optimal solution. This critical noise level monotonically increases with q and becomes even higher than that of some codes of connectivity $C = 3$, while the optimal decoding performance is inferior to that of $C = 3$ codes with the same q value. This may elucidate the role played by $C = 2$ components in irregular constructions.

Future directions include extending the analysis to irregular Gallager codes as well as to regular and irregular MN code [7, 6] in the Galois representation.

We acknowledge support from the RFTF program of the JSPS (YK), EPSRC (GR/N00562) and The Royal Society (DS).

REFERENCES

- [1] C. Berrou, A. Glavieux and P. Thitimajshima, in Proc. 1993 IEEE International Conference on Communications, Geneva, Switzerland, 1064 (1993).
- [2] M. C. Davey and D. J. C. Mackay, IEEE Comm. Lett., 2, 165 (1998).
- [3] R. G. Gallager, IRE Trans. Info. Theory, IT-8, 21 (1962).
- [4] Y. Iba, J. Phys. A: Math. and Gen., 32, 3875 (1999).
- [5] Y. Kabashima and D. Saad, Europhys. Lett., 44, 668 (1998); 45, 97 (1999).
- [6] Y. Kabashima, T. Murayama and D. Saad, Phys. Rev. Lett., 84, 1355 (2000); T. Murayama, Y. Kabashima, D. Saad and R. Vicente, Phys. Rev. E, 62, 1577 (2000).
- [7] D. J. C. Mackay, IEEE Trans. on Info. Theor., 45, 399 (1999); D. J. C. Mackay and R. M. Neal, Electronic Lett., 33, 457 (1997).
- [8] H. Nishimori, J. Phys. Soc. of Japan, 62, 2973 (1993).
- [9] P. Rujan, Phys. Rev. Lett., 70, 2968 (1993).
- [10] C. E. Shannon, Bell Sys. Tech. J., 27, 379 (1948); 27, 623 (1948).
- [11] N. Sourlas, Nature, 339, 693 (1989).
- [12] N. Sourlas, Euro. Phys. Lett., 25, 159 (1994).
- [13] R. Vicente, D. Saad and Y. Kabashima, J. Phys. A: Math. and Gen., 33, 1527 (2000).